Repeated Voltage Biasing Improves Unit Recordings by Reducing Resistive Tissue Impedances

Matthew D. Johnson, *Member, IEEE*, Kevin J. Otto, *Member, IEEE*, and Daryl R. Kipke, *Member, IEEE*

***Abstract*—Reactive tissue encapsulation of chronically implanted microelectrode probes can preclude long-term recording of extracellular action potentials. We investigated an intervention strategy for functionally encapsulated microelectrode sites. This method, known as "rejuvenation," involved applying a +1.5 V dc bias to an iridium site for 4 s. Previous studies have demonstrated that rejuvenation resulted in higher signal-to-noise ratios (SNRs) by decreasing noise levels, and reduced 1-kHz site impedances by decreasing the tissue interface resistances. In this study, we have investigated: 1) the duration of a single-voltage bias session and 2) the efficacy of multiple sessions. These questions were addressed through electrophysiological recordings, cyclic voltammetry, and modeling the electrode-tissue interface via an equivalent circuit model fit to impedance spectroscopy data. In the six implants studied, we found SNRs improved for 1–7 days with a peak typically occurring within 24 h of the voltage bias. Root-mean square (RMS) noise of the extracellular recordings decreased for 1–2 days, which paralleled a similar decrease in the adsorbed tissue resistance ($\mathrm{R_{en}}$) from the model. Implants whose SNR effects lasted more than a day showed stabilized reductions in the extracellular tissue resistance ($\mathrm{R_{ex}}$) and cellular membrane area ($\mathrm{A_m}$). Subsequent stimulus sessions were found to drop neural tissue parameters consistently to levels observed immediately after surgery. In most cases, these changes did parallel an improvement in SNR. These findings suggest that rejuvenation may be a useful intervention strategy to prolong the lifetime of chronically implanted microelectrodes**

***Index Terms*—Bias voltage, chronic recording, iridium, microelectrode, neuroprosthesis.**

I. Introduction

CHRONIC neural recording systems with extended functional lifetimes are essential for the field of neuroprostheses [1]–[7]. Realizing chronic systems that can record single and multiunit activity over periods of months to years, however, has been limited by reactive tissue encapsulation of the implant [4], [8], [9]. Studies have shown that microglia, astrocytes, and extracellular matrices can form encapsulation layers and in some cases electrically shield a neural probe's electrode sites from healthy neural tissue [10], [11]. The reactive tissue response at the neural interface includes both an early anti-inflammatory response due to insertion trauma and a sustained response induced in part by the interplay among micromotion [12], tethering [10], and device biocompatibility [9], [13].

In order to limit the early response, several improvements to insertion techniques and probe designs have been reported, including pneumatic probe insertion devices [14] and optimization of probe tip and shaft geometry [15]. Additionally, several methods have been proposed to inhibit the late reactive tissue response, including flexible probe substrates and ribbon cables [16], [17], bioactive factors [1], [18], [19], and peripheral and local delivery of anti-inflammatory drugs [20]. Once an electrode site becomes functionally encapsulated, however, there is a notable paucity of intervention strategies. We, and others, have shown previously that applying a +1.5 V bias for a few seconds, at a high impedance iridium electrode site with no sortable extra-cellular unit activity, can "rejuvenate" extra-cellular recording quality and lower site impedances [21]–[23]. While previous results suggest that this so-called "rejuvenation" procedure has promise, its long-term efficacy has not been investigated.

In this study, we have used chronic extra-cellular unit recordings and *in vivo* electrochemical measurements fit to an equivalent circuit model of the neural interface. We have compared these parameters across days to evaluate the long-term efficacy of voltage biasing for an initial session and for multiple sessions.

II. Methods

A. Device and Surgical Implantation

Six male Sprague–Dawley rats (250–300 g) were chronically implanted with silicon-substrate microelectrode arrays as described previously [23]. Briefly, the arrays consisted of four 50 μm-wide thin-film silicon shanks separated by 200 μm. Each shank contained four iridium microelectrodes (703-μm^2 site sizes) with 200-μm spacings between sites. In four rats, a single array was surgically implanted in the forelimb region of the primary motor cortex (M1). In two rats, two arrays were inserted into M1. All procedures complied with the guidelines for the care and use of laboratory animals and were approved by the University of Michigan Committee on Use and Care of Animals.

B. Rejuvenation Protocol

Rats with chronically implanted arrays were screened for microelectrode sites with 1-kHz impedances greater than 1 MΩ and little discernable extra-cellular unit activity. With the exception of S6 (see Table I), the rejuvenation protocol began at

Manuscript received December 8, 2004; revised February 15, 2005; accepted February 21, 2005. This work was supported in part by the Defense Advanced Research Projects Agency under Grant N66001-02-C-8059, in part by the Center for Neural Communication Technology under Grant P41-EB00230, and in part by the Engineering Research Centers program of the National Science Foundation (NSF) under NSF Award Number EEC-9986866.

M. D. Johnson and D. R. Kipke are with the Biomedical Engineering Department, University of Michigan, Ann Arbor, MI 48109 USA (e-mail: mdjzz@umich.edu; dkipke@umich.edu).

K. J. Otto is with the Kresge Hearing Research Institute, University of Michigan, Ann Arbor, MI 48109 USA (e-mail: kjotto@umich.edu).

Digital Object Identifier 10.1109/TNSRE.2005.847373

TABLE I
PROTOCOL FOR EACH RAT

Subjects (day post-implant of first DC bias)	Arrays (rejuvenated / control sites)	Experiment	DC Bias Sessions
S1: bmi16 (97)	A (14/0) & B (10/4)	LONG; MULT	3
S2: bmi24 (33)	A (7/5) & B (8/8)	LONG; MULT	2
S3: kcd01 (26)	(14/0)	LONG; MULT	7
S4: ottobmi6 (33)	(14/0)	LONG	1
S5: kcd9 (24)	(16/0)	MULT	9
S6: kcd10 (10)	(16/0)	MULT	9

NOTE: LONG – long-term efficacy of a single rejuvenation session; MULT – efficacy of multiple rejuvenation sessions

least three weeks after the surgical implantation, allowing for the early tissue response to peak and stabilize [9].

Voltage biasing involved applying a single 4-s, +1.5-V dc pulse to an iridium microelectrode site in reference to a bone screw. Resulting current was sampled by an Autolab potentiostat PGSTAT12 (Eco Chemie, Utrecht, The Netherlands) at 1 Hz with currents in the 100–200-nA range. During this procedure, the animal was awake and resting in a faraday cage. Multiple voltage biasing sessions occurred over a two month period on arrays in five rats. In a set of three implants, certain "control" sites were not stimulated.

C. Electrophysiological Recordings

In four rats (S1–4), extra-cellular unit recordings were made before, immediately after (within 1 h), and for the subsequent week following each rejuvenation. The recordings consisted of voltage-time series data sets sampled at 40 kHz on a multichannel acquisition processor (Plexon Inc., Dallas, TX) for 30 s and repeated 2–6 times per day [23]. During recording sessions, the rats were awake and sitting quietly in an electrically and acoustically shielded chamber. The electrophysiological data were analyzed offline using custom software in Matlab (Mathworks, Natick, MA). An objective measure of signal quality was made using a wavelet analysis method to estimate noise amplitude, signal amplitude, and signal-to-noise ratio (SNR) [24].

D. Electrochemical Techniques

Electrochemical impedance spectroscopy (EIS) and cyclic voltammetry (CV) measurements were made on chronically implanted arrays using an Autolab potentiostat with a built-in frequency response analyzer (Brinkmann, Westbury, NY). A bone screw, composed of stainless steel 316SS-grade, served as the reference during electrochemical measurements. The 316SS grade has been shown to be resistant to corrosion and capable of providing a stable reference potential *in vivo* [25].

Prior to and for one week after rejuvenation, EIS and CV measurements were performed. EIS involved applying a 25-mV RMS sine wave with frequencies ranging from 0.1 to 10 kHz. These measurements provided data to analyze changes in electrode and tissue properties through a neural interface model. CV measurements used a linear sweeping voltage between −0.25 V and +0.75 V with a 1 V/s scan rate. For each electrode site, the resulting forward scan of the voltammagram was integrated to determine the charge capacity (Q_{cap}).

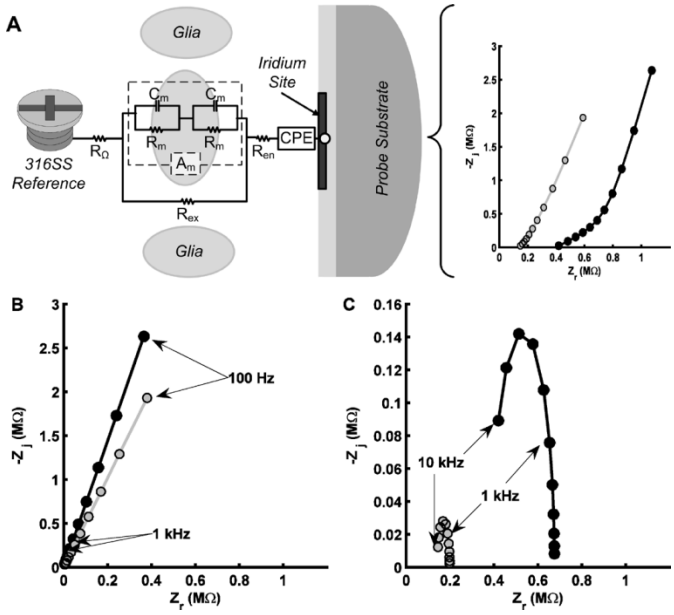

Fig. 1. Iterative algorithm decoded impedance spectroscopy data into neural interface parameters represented by an equivalent circuit model. (A) The model included an iridium microelectrode, an adsorbed resistive layer, and a reactive glial layer. (B) A Nyquist plot of the decoded electrode component showed that rejuvenation resulted in a slight enhancement to the electrode conductivity (pre-rejuvenation: black line; post-rejuvenation: gray). (C) A Nyquist plot of the decoded tissue components demonstrated that rejuvenation induced a substantial decrease in the resistive components of the tissue interface ($R_{en} + R_{ex}$), especially at 1 kHz.

E. Neural Interface Model

An equivalent circuit model of the electrode-tissue interface was developed and histologically verified to describe tissue reaction at a microwire electrode after chronic implantation [26]. This paper applied the model to evaluate effects of bias voltage on the neural interface *in vivo*. The circuit model [Fig. 1(a)] included an iridium microelectrode component and a neural tissue component determined by characteristics of the encapsulation phenomenon [11]. See [23] for model details.

Briefly, the electrode component was modeled with a constant phase element CPE [(1)], which consisted of a gain term (K) and a phase term (α) defined $0 \leq \alpha \leq 1$

$$Z_{CPE} = \frac{K}{(j\omega)^{\alpha}}. \tag{1}$$

A constant phase element was sufficient to describe the nonideal double-layer capacitance behavior of iridium during impedance measurements [27].

The tissue encapsulation of the array was characterized by a sealing resistance (R_{en}), describing protein adsorption and in some cases a layer of connective tissue [28]–[30]. In addition, the model incorporated adjacent cellular layers of glia and macrophages given by a membrane capacitance ($C_m = 1 \times 10^{-6}\ \mu F/cm^2$), a membrane conductance ($g_m = 0.3\ S/cm^2$), and a membrane area scaling term (A_m) [28]. The extracellular pathway between cells was defined as a resistance (R_{ex}). A measured shunt capacitance of 10 pF was also included in the model. The spreading resistance (R_Ω) from the cellular circuit to the counter electrode was assumed negligible given the relatively

large surface area of the bone screw. Finally, lead wire resistances were minimal ($< 3\ \Omega$) and, therefore, neglected.

Using a nonlinear regression paradigm, we developed an algorithm to utilize complex impedance spectroscopy measurements and estimate equivalent circuit components by iteratively fitting high and low frequency data points to their respective circuit pathways [Fig. 1(b)–(c)]. Obtaining an optimal fit involved minimizing an objective function J

$$J = \sum_k \frac{\left(Zr_k - \hat{Z}r_k\right)^2}{{w_k}^2} + \sum_k \frac{\left(Zj_k - \hat{Z}j_k\right)^2}{{w_k}^2} \qquad (2)$$

where Zr_k and Zj_k are the real and imaginary data, respectively; $\hat{Z}r_k$ and $\hat{Z}j_k$ represent the model fit; and w_k is a weight given by the impedance magnitude $|\mathrm{Z}_k|$ at a given frequency. Incorporating weights was important to prevent biasing J to low-frequency data. Parameter estimations that did not fit a $0.95\mathrm{R}^2$ measure were discarded.

III. Results

A. Long-Term Evaluation of a Rejuvenation Session

Previously, we investigated the effects within 1 h of rejuvenation and found significant increases in SNRs as well as significant decreases in encapsulated tissue resistances [23]. We now have examined the functional duration of these effects for the first voltage bias session and correlated changes in interface parameters with electrophysiological recordings.

In the six implants studied, electrophysiological recording quality increased significantly within 1 h of the first voltage bias session, (paired t-test, $\mathrm{p} < 0.001$, $\mathrm{n} = 67$). For nonstimulated control sites, SNRs did not increase significantly, (paired t-test, $\mathrm{p} = 0.065$, $\mathrm{n} = 17$). Week-long recording trends in biased and control sites for the S1B implant are shown in Fig. 2(A)–(C).

Increased recording quality varied in duration among implants: less than 24 h in four cases (S1A,B and S2A,B), three days in one case (S3), and seven days in the another case (S4) (one-way ANOVA, $\mathrm{p} < 0.05$ for significant days). An example of the week-long trends in SNR for arrays whose signal quality improved for one day (S1B) and for seven days (S4) is shown in Fig. 2(D). The highest measured SNRs typically occurred immediately after the voltage bias. These peaks corresponded to significant reductions in RMS noise, decreasing on average by 23.0% for S1B and 26.7% for S4 [Fig. 2(E)]. Recording noise returned to pre-rejuvenation levels within two days for both implants (one-way ANOVA, $\mathrm{p} > 0.05$ on day two). Differences between arrays were evident in the analysis of signal amplitudes as shown in Fig. 2(F). The average signal amplitude measured by arrays in S4, for instance, increased steadily after rejuvenation.

We next applied the neural interface model algorithm to impedance spectroscopy data collected over the same week-long period. In terms of the electrode properties, the gain (K) and phase (α) were found to decrease after the stimulus [Fig. 3(a)–(b)]. For both arrays in S1, K and α remained significantly reduced for seven days on biased sites (one-way ANOVA, $\mathrm{F} = 21.32$, $\mathrm{p} < 0.001$ on day seven). In contrast to

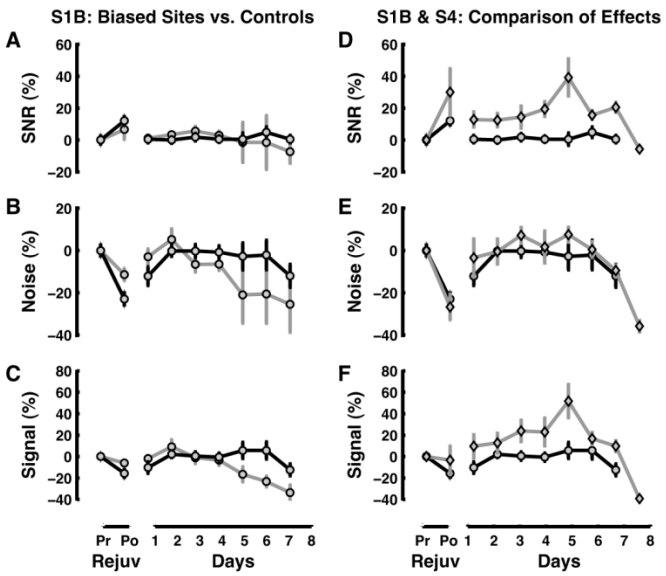

Fig. 2. Voltage biasing caused 1 to 7-day increases in unit recording SNRs. (A)-(C) Larger SNRs were observed on voltage biased sites (black line) over controls (gray line) due to significantly less noise on biased sites. (D)-(F) Typically, the highest SNR was observed immediately after the stimulus as shown for arrays in both S1B (black line) and S4 (gray line). In contrast to the 1-day noise reduction for both arrays, signal amplitude increased steadily for 1-week only in S4. Error bars represent standard errors.

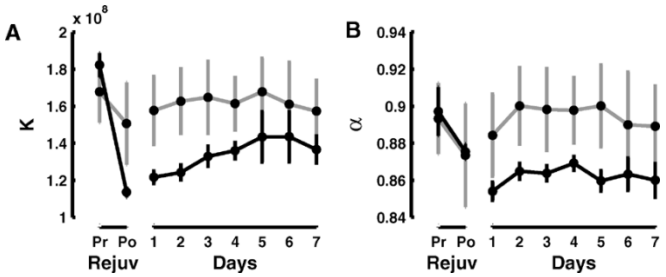

Fig. 3. Voltage biasing caused site-specific, week-long enhancements to electrode conductivity. A representative example from arrays in S1 showed prolonged, reduced levels in both (A) the electrode gain K and (B) the electrode phase α. Black traces represent rejuvenated sites in S1 ($\mathrm{n} = 24$); gray traces signify nonrejuvenated sites ($\mathrm{n} = 4$). Pr: Pre-rejuvenation. Po: Post-rejuvenation. Error bars represent standard errors.

α, however, K was found to return to its pre-rejuvenation value after three weeks (one-way ANOVA, $\mathrm{F} = 1.86$ $\mathrm{p} = 0.18$ on day 23). Changes in electrode parameters for control sites were not apparent.

The only decoded tissue parameter to change on control sites was the sealing resistance R_{en} [for example, Fig. 4(A)–(C)]. For voltage biased sites in all implants, R_{en} decreased by 49.1% on average (one-way ANOVA, $\mathrm{F} = 131$, $\mathrm{p} < 0.001$, $\mathrm{n} = 51$ pre- and $\mathrm{n} = 62$ post-biasing). However, this attenuation was transient, returning to its pre-rejuvenation level within 1–2 days, as shown for S1B and S4 in Fig. 4(D). In contrast, the array implanted in S4 showed significantly lower relative values for R_{ex} after seven days (S1B: 1.702 $\mathrm{M}\Omega$ and S4: 168 $\mathrm{k}\Omega$) [see Fig. 4(E)]. The cellular membrane area term A_{m} for both arrays decreased significantly following rejuvenation. Similar to the R_{ex} term, A_{m} remained steadily below its pre-rejuvenation value [Fig. 4(F)].

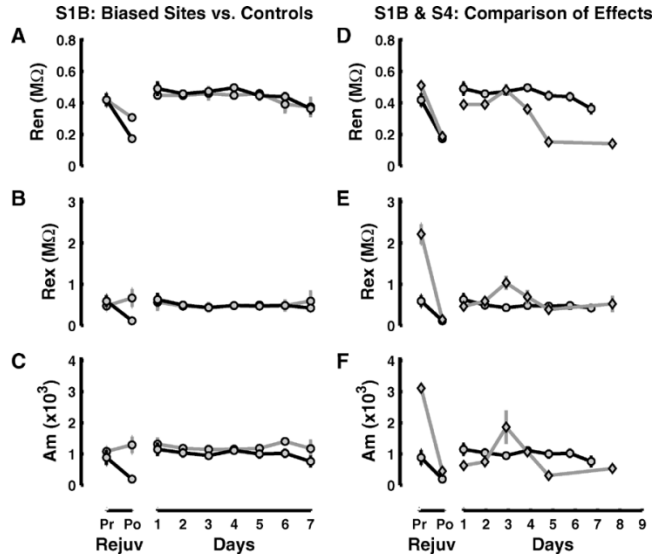

Fig. 4. Voltage biasing caused transient changes to neural interface properties lasting 1–7 days. (A)-(C) Model parameter $\mathrm{R_{en}}$ decreased for both voltage biased (black line: $\mathrm{n} = 12$) and control (gray line: $\mathrm{n} = 4$) electrode sites, whereas biasing was site-specific for $\mathrm{R_{ex}}$ and $\mathrm{A_m}$. (D)-(F) In comparison to the S1B implant (black line: $\mathrm{n} = 12$), array sites in S4 (gray line: $\mathrm{n} = 12$) showed significantly smaller $\mathrm{R_{en}}$ values after one week. In addition, parameters $\mathrm{R_{ex}}$ and $\mathrm{A_m}$ remained significantly attenuated after one week for the array in S4. Pr: Pre-rejuvenation. Po: Post-rejuvenation. Note that error bars represent standard errors, some of which are very small.

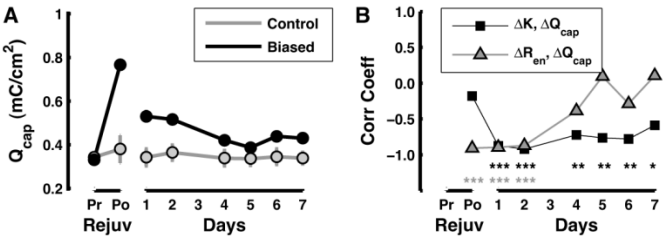

Fig. 5. Charge capacity ($\mathrm{Q_{cap}}$) measurements captured neural interface parameter variations. (A) For biased sites in both S1 implants, $\mathrm{Q_{cap}}$ peaked and stabilized at an elevated level for one-week. Black ($\mathrm{n} = 22$) and gray ($\mathrm{n} = 4$) traces correspond to biased and control sites, respectively. Error bars represent standard errors. (B) The transient peak in $\mathrm{Q_{cap}}$ correlated with change in Ren, whereas change in the electrode gain K correlated with the week-long elevated level in $\mathrm{Q_{cap}}$ (***: $\mathrm{p} < 0.001$. **: $\mathrm{p} < 0.01$. *: $\mathrm{p} < 0.05$).

The charge capacity ($\mathrm{Q_{cap}}$) calculations from *in vivo* CV measurements captured both the sustained electrode conductivity and the more transient tissue impedance changes, as shown for arrays in S1 [Fig. 5(A)]. $\mathrm{Q_{cap}}$ increased significantly after biasing (132%, ANOVA, $\mathrm{F} = 658.5$, $\mathrm{p} < 0.001$, $\mathrm{n} = 22$) and sustained an elevated level for one week (27%, ANOVA, $\mathrm{F} = 12.3$, $\mathrm{p} = 0.001$, $\mathrm{n} = 22$). The peak increase in charge capacity immediately after biasing correlated with a decrease in $\mathrm{R_{en}}$ ($\mathrm{r} = -0.91$, ANOVA, $\mathrm{F} = 70.32$, $\mathrm{p} < 0.001$, $\mathrm{n} = 17$ for sites with both measurements) [see Fig. 5(B)]. The only neural interface parameter to correlate with long term trends in $\mathrm{Q_{cap}}$ was K ($\mathrm{r} = -0.59$, ANOVA, $\mathrm{F} = 6.85$, $\mathrm{p} = 0.021$, $\mathrm{n} = 15$ on day seven). Finally, the increase in RMS noise on day one correlated with an increase in $\mathrm{R_{en}}$ ($\mathrm{r} = 0.91$, ANOVA, $\mathrm{F} = 63.1$, $\mathrm{p} < 0.001$, $\mathrm{n} = 17$) and $\mathrm{Q_{cap}}$ ($\mathrm{r} = -0.89$, ANOVA, $\mathrm{F} = 46.7$, $\mathrm{p} < 0.001$, $\mathrm{n} = 17$).

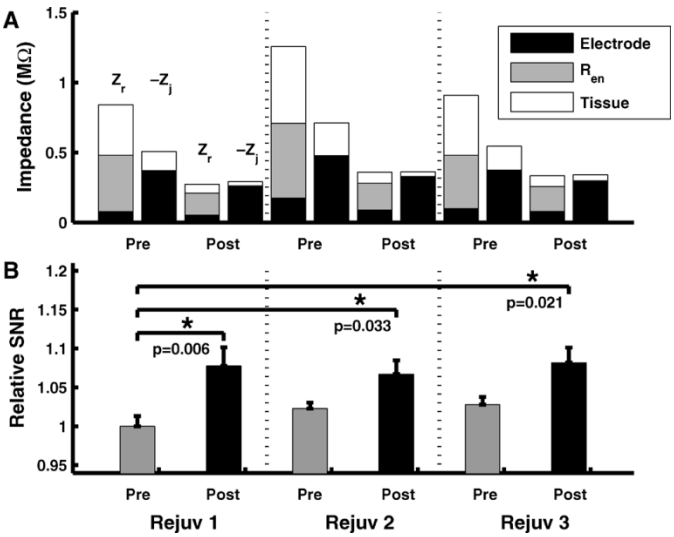

Fig. 6. In S1, voltage bias sessions occurred 97, 121, and 131 days after surgical implantation. (A) Each session caused a significant decrease in neural interface parameters, represented by real ($\mathrm{Z_r}$) and imaginary ($-\mathrm{Z_j}$) 1 kHz impedance data. The most significant drops occurred in $\mathrm{R_{en}}$ and the resistive components of the tissue. (B) The most significant improvement in SNR typically occurred at the first rejuvenation; however, some subsequent sessions were able to increase signal quality significantly above the pre-rejuvenation level. Error bars represent standard errors.

B. Evaluation of Repeated Voltage Biasing

Given that rejuvenation caused a transitory enhancement in neural interface conductivity and SNR, we tested whether repeated voltage bias sessions would be as effective as the initial treatment. Five rats underwent multiple voltage bias sessions over the course of two months. In two rats (S5 and S6) only 1-kHz impedances were measured.

Each of the 29 sessions was found to be effective at decreasing the 1 kHz impedance from an average of 1.921 ± 0.049 MΩ to 0.795 ± 0.033 MΩ (one-way ANOVA, $\mathrm{p} < 0.001$, $\mathrm{n} = 385$). In terms of the neural interface model, the most substantial and consistent impedance decrease came from the sealing resistance $\mathrm{R_{en}}$ and the cellular layers, particularly the resistive component, $\mathrm{R_{ex}}$. For the rat shown in Fig. 6(A), each of the three sessions reduced $\mathrm{R_{en}}$ (by 246, 337, and 203 kΩ) and $\mathrm{R_{ex}}$ (379, 634, and 456 kΩ). While the mean impedance of the electrode component did decrease after each session (112, 167, 79 kΩ), the magnitude of the change was smaller than the changes in $\mathrm{R_{en}}$ and $\mathrm{R_{ex}}$. In general, neural interface parameters were not found to increase appreciably beyond values measured prior to the first voltage bias session.

In most cases, decreases in neural interface parameters paralleled an improvement in SNR [Fig. 6(B)]. The most significant percentage increase in signal quality typically resulted from the first session. After each of the three bias sessions for arrays in S1, RMS noise decreased by 23.7%, 8.7%, and 9.8%, respectively. Signal amplitude was reduced on the first rejuvenation by 16.6%, but subsequent rejuvenations did not change it significantly. In three rats undergoing multiple rejuvenations ($\mathrm{n} = 2$, $\mathrm{n} = 3$, $\mathrm{n} = 7$), we observed significant increases in SNR beyond the first pre-stimulus level on subsequent sessions. However, on the sixth and seventh sessions in S3, we

observed degradation in the spiking signal strength leading to poor signal-to-noise ratios.

IV. Discussion

In this study, we evaluated the long-term effects of single and multiple voltage bias sessions in terms of both extracellular recording quality and neural interface parameters. In terms of recordings, noise remained attenuated for 1–2 days following a session, with the return to baseline correlating with the model's metric for material adsorbed to the electrode surface ($\mathrm{R_{en}}$) and the charge capacity parameter ($\mathrm{Q_{cap}}$). In contrast, signal amplitude changes induced by rejuvenation had varying durations among rats. Prolonged enhancements in unit recording SNR corresponded to larger signal amplitudes over the week-long period. This observation paralleled a similarly prolonged decrease in the extracellular resistance ($\mathrm{R_{ex}}$) and membrane area ($\mathrm{A_m}$) components. In contrast, the electrode conductivity enhancements, measured in K and α, lasted at least one week. This enhancement, previously demonstrated *in vitro*, was consistent with the formation of a monolayer of anodic hydrous iridium oxide [31]. The electrochemically observed monolayer degradation after many weeks *in vivo* calls for further investigation.

Multiple voltage bias sessions over months were found to decrease 1-kHz site impedances and neural interface parameters to levels comparable with those measured after the first session. In most cases, these changes did parallel an improvement in SNR; however, in one of the arrays, biasing induced degradation in signal quality on two sessions. This suggests that rejuvenation by itself may not be a universal, permanent solution to enable long-term chronic unit recordings. In some cases, however, it may be effective. Local infusion of chemical agents to maintain changes in the neural interface after rejuvenation may lengthen and sustain the improvement in SNR [32].

The results suggest that rejuvenation increased unit recording quality by creating transient conductivity pathways through the encapsulated sheath of nonneuronal tissue surrounding a probe implant. Despite *in vivo* changes to the neural interface following rejuvenation, for the most part, model components did not deteriorate beyond their pre-rejuvenation values. This suggests that voltage biasing may not compound the implant encapsulation. In future studies, histology of the explanted brains will be used to corroborate these findings from our neural interface model.

The neural interface model utilized in these studies has been well-characterized through both *in vitro* culturing of cells on electrode sites [28] and correlation of *in vivo* microwire electrode measurements with immunohistochemistry [26]. In addition to these studies, the long-term cyclic voltammetry data corroborates the findings that adsorption of tissue on the electrode surface is a dominant factor in observed SNRs. Though the model lacks spatial specificity, we can be reasonably confident that the impedance measurements describe the underlying encapsulation phenomena, which is typically 10–100 μm thick [20]. From microelectrode theory, we know that 50% of the interface impedance lies within 30 μm of the electrode site and 90% of the impedance is within 250 μm [26]. The model thus predicts parameters that can inhibit neuronal signal propagation [33].

V. Conclusion

We investigated the duration of electrophysiological recording quality enhancement following a single-voltage bias session and correlated the measurements with decoded values from a model of the neural interface. Our findings indicate that the effects of a single "rejuvenation" session typically last less than one week, characterized by transient changes in tissue and prolonged changes in electrode properties. Multiple stimulus sessions over a two-month period demonstrated that in some cases repeated biasing can re-enhance unit recording SNR. This analysis suggests that rejuvenation can be a useful intervention strategy for chronically implanted iridium microelectrodes.

Acknowledgment

The authors would like to thank J. Williams for discussion related to model development, G. Gage for surgical assistance, and the Neural Engineering Laboratory for discussion on the manuscript. The authors would also like to thank J. Hetke and the CNCT for fabricating and assembling the neural probes.

References

[1] P. R. Kennedy, "The cone electrode: A long-term electrode that records from neurites grown onto its recording surface," *J. Neurosci. Methods*, vol. 29, pp. 181–193, 1989.

[2] P. J. Rousche and R. A. Normann, "Chronic recording capability of the utah intracortical electrode array in cat sensory cortex," *J. Neurosci. Meth.*, vol. 82, pp. 1–15, 1998.

[3] J. C. Williams, R. L. Rennaker, and D. R. Kipke, "Long-term neural recording characteristics of wire microelectrode arrays implanted in cerebral cortex," *Brain Res. Protoc.*, vol. 4, pp. 303–313, 1999.

[4] X. Liu, D. B. McCreery, R. R. Carter, L. A. Bullara, T. G. Yuen, and W. F. Agnew, "Stability of the interface between neural tissue and chronically implanted intracortical microelectrodes," *IEEE Trans. Rehab. Eng.*, vol. 7, no. 3, pp. 315–326, Sep. 1999.

[5] D. R. Kipke, R. J. Vetter, J. C. Williams, and J. F. Hetke, "Silicon-substrate intracortical microelectrode arrays for long-term recording of neuronal spike activity in cerebral cortex," *IEEE Trans. Neur. Sys. Rehab.*, vol. 11, no. 2, pp. 151–155, Jun. 2003.

[6] M. A. Nicolelis, D. Dimitrov, J. M. Carmena, R. Crist, G. Lehew, J. D. Kralik, and S. P. Wise, "Chronic, multisite, multielectrode recordings in macaque monkeys," in *Proc. Nat. Acad. Sci., U.S.A.*, vol. 100, 2003, pp. 11 041–11 046.

[7] R. J. Vetter, J. C. Williams, J. F. Hetke, E. A. Nunamaker, and D. R. Kipke, "Chronic neural recording using silicon-substrate microelectrode arrays implanted in cerebral cortex," *IEEE Trans. Biomed. Eng.*, vol. 51, no. 6, pp. 896–904, Jun. 2004.

[8] D. H. Szarowski, M. D. Andersen, S. Retterer, A. J. Spence, M. Isaacson, H. G. Craighead, J. N. Turner, and W. Shain, "Brain responses to micromachined silicon devices," *Brain Res.*, vol. 983, pp. 23–35, 2003.

[9] J. N. Turner, W. Shain, D. H. Szarowski, M. Andersen, S. Martins, M. Isaacson, and H. Craighead, "Cerebral astrocyte response to micromachined silicon implants," *Exp. Neurol.*, vol. 156, pp. 33–49, 1999.

[10] Y. T. Kim, R. W. Hitchcock, M. J. Bridge, and P. A. Tresco, "Chronic response of adult rat brain tissue to implants anchored to the skull," *Biomaterials*, vol. 25, pp. 2229–2237, 2004.

[11] S. S. Stensaas and L. J. Stensaas, "Reaction of cerebral-cortex to chronically implanted plastic needles," *Acta Neuropathol.*, vol. 35, pp. 187–203, 1976.

[12] J. Subbaroyan, D. C. Martin, and D. R. Kipke, "A finite-element model of the mechanical effects of implantable microelectrodes in the cerebral cortex," *J. Neural Eng.*, to be published.

[13] S. S. Stensaas and L. J. Stensaas, "Histopathological evaluation of materials implanted in cerebral-cortex," *Acta Neuropathol.*, vol. 41, pp. 145–155, 1978.

[14] P. J. Rousche and R. A. Normann, "A method for pneumatically inserting an array of penetrating electrodes into cortical tissue," *Ann. Biomed. Eng.*, vol. 20, pp. 413–422, 1992.

[15] D. J. Edell, V. V. Toi, V. M. McNeil, and L. D. Clark, "Factors influencing the biocompatibility of insertable silicon microshafts in cerebral cortex," *IEEE Trans. Biomed. Eng.*, vol. 39, no. 6, pp. 635–643, Jun. 1992.
[16] P. J. Rousche, D. S. Pellinen, D. P. Pivin, J. C. Williams, R. J. Vetter, and D. R. Kipke, "Flexible polyimide-based intracortical electrode arrays with bioactive capability," *IEEE Trans. Biomed. Eng.*, vol. 48, no. 3, pp. 361–371, Mar. 2001.
[17] J. F. Hetke, J. L. Lund, K. Najafi, K. D. Wise, and D. J. Anderson, "Silicon ribbon cables for chronically implantable microelectrode arrays," *IEEE Trans. Biomed. Eng.*, vol. 41, no. 4, pp. 314–321, Apr. 1994.
[18] X. Cui, V. A. Lee, Y. Raphael, J. A. Wiler, J. F. Hetke, D. J. Anderson, and D. C. Martin, "Surface modification of neural recording electrodes with conducting polymer/biomolecule blends," *J. Biomed. Mater. Res.*, vol. 56, pp. 261–272, 2001.
[19] Y. Zhong, X. Yu, R. Gilbert, and R. V. Bellamkonda, "Stabilizing electrode-host interfaces: A tissue engineering approach," *J. Rehab. Res. Dev.*, vol. 38, pp. 627–632, 2001.
[20] W. Shain, L. Spataro, J. Dilgen, K. Haverstick, S. Retterer, M. Isaacson, M. Saltzman, and J. N. Turner, "Controlling cellular reactive responses around neural prosthetic devices using peripheral and local intervention strategies," *IEEE Trans. Neural Syst. Rehab. Eng.*, vol. 11, no. 2, pp. 186–188, Jun. 2003.
[21] K. D. Wise, "Chronic implantation of passive probes," in *NIH Neural Prosthesis Program QPR2*, 1991, pp. 22–24.
[22] E. M. Schmidt, W. J. Heetderks, and D. M. Camesi-Cole, "Chronic neural recording with multicontact silicon microprobes: Effects of electrode bias," *Soc. Neurosci.*, p. 982, 1994.
[23] K. J. Otto, M. D. Johnson, and D. R. Kipke, "Bias voltages change neural interface properties and improve unit recordings with chronically implanted microelectrodes," *IEEE Trans. Biomed. Eng.*, to be published.
[24] A. E. Snellings, J. W. Aldridge, and D. J. Anderson, "Use of multichannel recording electrodes and independent component analysis for isolating neural signals," in *Soc. Neurosci.*, 2003, Program No. 429.6.
[25] J. D. Weiland and D. J. Anderson, "Chronic neural stimulation with thin-film, iridium oxide electrodes," *IEEE Trans. Biomed. Eng.*, vol. 47, no. 7, pp. 911–918, Jul. 2000.
[26] J. C. Williams, *Performance of Chronic Neural Implants*. Tempe, AZ: Arizona State Univ., 2001.
[27] E. T. McAdams, A. Lackermeier, J. A. Mclaughlin, D. Macken, and J. Jossinet, "The linear and nonlinear electrical-properties of the electrode-electrolyte interface," *Biosens. Bioelectron.*, vol. 10, pp. 67–74, 1995.
[28] J. R. Buitenweg, W. L. Rutten, W. P. Willems, and J. W. van Nieuwkasteele, "Measurement of sealing resistance of cell-electrode interfaces in neuronal cultures using impedance spectroscopy," *Med. Biol. Eng. Comput.*, vol. 36, pp. 630–637, 1998.
[29] R. B. Stein, D. Charles, T. Gordon, J. A. Hoffer, and J. Jhamandas, "Impedance properties of metal electrodes for chronic recording from mammalian nerves," *IEEE Trans. Biomed. Eng.*, vol. BME-25, no. 6, pp. 532–537, Jun. 1978.
[30] W. M. Grill and J. T. Mortimer, "Electrical properties of implant encapsulation tissue," *Ann. Biomed. Eng.*, vol. 22, pp. 23–33, 1994.
[31] P. G. Pickup and V. I. Birss, "A model for anodic hydrous oxide-growth at iridium," *J. Electroanal. Chem.*, vol. 220, pp. 83–100, 1987.
[32] S. T. Retterer, K. L. Smith, C. S. Bjornsson, K. B. Neeves, A. J. Spence, J. N. Turner, W. Shain, and M. S. Isaacson, "Model neural prosthesis with integrated microfluidics: A potential intervention strategy for controlling reactive cell and tissue responses," *IEEE Trans. Biomed. Eng.*, vol. 51, no. 11, pp. 2063–2073, Nov. 2004.
[33] D. A. Henze, Z. Borhegyi, J. Csicsvari, A. Mamiya, K. D. Harris, and G. Buzsaki, "Intracellular features predicted by extracellular recordings in the hippocampus in vivo," *J. Neurophysiol.*, vol. 84, pp. 390–400, 2000.

Matthew D. Johnson (M'03) received the S.B. degree in engineering sciences from Harvard University, Cambridge, MA, in 2002, and the M.S. degree in biomedical engineering in 2003 from the University of Michigan, Ann Arbor, where he is currently working toward the Ph.D. degree in biomedical engineering.

From 2000 to 2002, he was a Research Assistant in the Harvard BioControls Laboratory, where his work was in the area of telemetry and neural engineering. From 2002 to the present, he has been a Research Assistant in the Neural Engineering Laboratory, University of Michigan, Ann Arbor. His research interests include the application of BioMEMS to detect neurochemicals *in vivo* and the evaluation of chronically implanted neural probe microsystems.

Kevin J. Otto (M'03) received the B.S. degree in chemical engineering from Colorado State University, Fort Collings, in 1997, and the M.S. and Ph.D. degrees in bioengineering from Arizona State University, Tempe, in 2002 and 2003, respectively.

From 1997 to 2003, he was a Research Assistant with the Bioengineering Department, Arizona State University, where his work was in the areas of neural engineering and sensory neuroprostheses. From 2003 to 2004, he was a Research Fellow with the Department of Biomedical Engineering, University of Michigan, Ann Arbor, where his work focused on brain–machine interface systems and implantable devices. He is currently a Postdoctoral Fellow in the Central Systems Laboratory, Kresge Hearing Research Institute, Department of Otolaryngology, University of Michigan. His research interests include neuroprostheses, systems neuroscience, and neurotechnologies.

Daryl R. Kipke (S'87–M'90) received the B.Sc. degree in engineering science, the M.Sc. degree in bioengineering, the M.S.E. degree in electrical engineering, and the Ph.D. degree in bioengineering from the University of Michigan, Ann Arbor, in 1985, 1986, 1988, and 1991, respectively.

From 1991 to 1992, he was a Research Associate with the Department of Bioengineering and the Institute for Sensory Research at Syracuse University, Syracuse, NY. In 1992, he joined the Bioengineering Faculty at Arizona State University, Tempe. In 2001, he joined the Faculty of the College of Engineering, University of Michigan, where he is currently an Associate Professor in the Departments of Biomedical Engineering and Electrical Engineering and Computer Science, and directs the Neural Engineering Laboratory. His primary research interests include the areas of BioMEMS for neural implants, neuroprostheses, systems neuroscience, functional neurosurgery, and neurotechnologies. He teaches in the areas of biomedical instrumentation and neural engineering.

Dr. Kipke is a Fellow of the American Institute of Medical and Biological Engineering.